

Supplementary Information

for

Cation Templated Improved Synthesis of Pillar[6]arenes

Marta Da Pian,^a Ottorino De Lucchi^a, Giorgio Strukul,^a Fabrizio Fabris^{a,*} Alessandro Scarso^{a,*}

a) Dipartimento di Scienze Molecolari e Nanosistemi, Università Ca'Foscari di Venezia, Via Torino 155,

30172, Mestre Venezia (ITALY)

alesca@unive.it; fabrisfa@unive.it

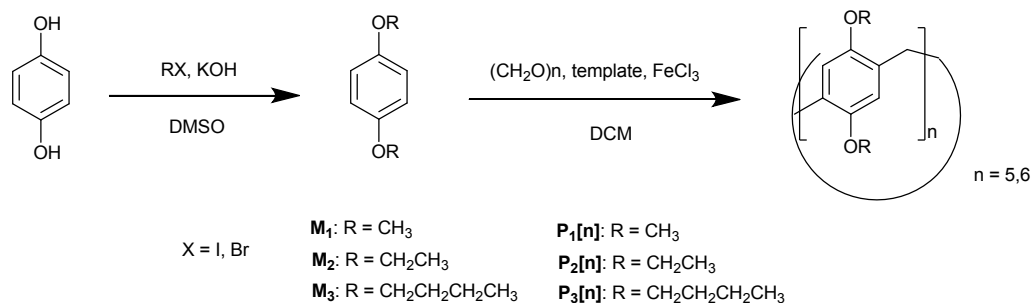
Contents:

Materials and method	S2
Synthesis of Dialkoxypillar[5]arenes and Dialkoxypillar[6]arenes	S2
¹ H NMR Spectra of Host-Guest Interaction of P ₂ [5] with T ₂ , T ₃ , T ₄	S15
¹ H NMR Spectra of Host-Guest Interaction of P ₂ [6] with T ₂ , T ₃ , T ₄	S16
ESI-MS Spectra of Host-Guest complex of P ₂ [5] with T ₄	S18
ESI-MS Spectra of Host-Guest complex of P ₂ [6] with T ₂ , T ₃	S18
Determination of the Kass between P ₂ [6] and T ₂	S19
Semiempirical PM3 calculations on T ₂ @P ₂ [5] and T ₂ @P ₂ [6]	S20

1. Materials and Method

Solvents used in the study were reagent grade and purchased from commercial national sources. Hydroquinone, ethyl iodide, methyl iodide, butylbromide, paraformaldehyde, FeCl_3 , tetramethylammoniumchloride, *bis*(cyclopentadienyl)Cobalt (III) hexafluorophosphate were reagent grade and purchased from Sigma-Aldrich. Deionized water was used in all experiments. ^1H and ^{13}C NMR spectra were collected on a Bruker-300 MHz NMR spectrometer. Low resolution electrospray ionization mass spectrometry LRMS (ESI-MS) experiments were carried out in positive mode with Agilent Technologies LC/MSD Trap SL AGILENT instrument (mobile phase Acetonitrile). (Ferrocenylmethyl)trimethylammonium hexafluorophosphate was synthesized and characterized according to literature procedures.^{S1}

2. Synthesis of Dialkoxypillar[5]arene and Dialkoxypillar[6]arene



Scheme S1. Synthesis of dialkoxy-benzenes^{S2} and the corresponding Pillar[n]arenes.

2.1 Synthesis of pillar[n]arenes in the presence of \mathbf{T}_1 or \mathbf{T}_4 . A mixture of FeCl_3 (0,048 g , 0,3 mmol) (and $\mathbf{T}_1/\mathbf{T}_4$ in a 1:2 molar ratio was heated at 100 °C with gentle stirring until a dark brown liquid was obtained. A solution of 1,4-dialkoxybenzene (0,166 g, 1 mmol), paraformaldehyde (0,091 g, 3 mmol) in dichloromethane (20 ml) was added to the mixture. After stirring at room temperature for 4h, the reaction was quenched by addition of water. The organic phase was separated and washed with saturated aqueous NaHCO_3 , water and brine. The crude product was purified by column chromatography (eluant: Cyclohexane (Cy)/dichloromethane (DCM) in gradient from 3:7 to 1:9). R_f of $\mathbf{P}[5]$ = 0.4 in 3:7 Cy/DCM; R_f of $\mathbf{P}[6]$ = 0.4 in 1:9 Cy/DCM.

2.2 Synthesis of pillar[n]arenes in the presence of T₂ or T₃. A mixture of FeCl₃ (50.3 mg, 0.3 mmol), T₂/T₃ (0.04 mmol), 1,4-dialkoxybenzene (1 mmol), paraformaldehyde (90 mg, 3 mmol) in dichloromethane (20 ml) was prepared. After stirring at room temperature for 4h, the reaction was quenched by addition of water. The organic phase was separated and washed with saturated aqueous NaHCO₃, water and brine. The crude product was purified by column chromatography (eluant: Cy/DCM in gradient from 3:7 to 1:9). R_f of P[5] = 0.4 in 3:7 Cy/DCM; R_f of P[6] = 0.4 in 1:9 Cy/DCM.

2.3 Characterization of Pillar[n]arenes

2.3.1 P₁[5].

¹H NMR (300 MHz, CDCl₃, 25 °C) δ (ppm): 6.75 (s, 10H), 3.77 (s, 10H), 3.73 (s, 30H). ¹³C NMR (300 MHz, CDCl₃, 25 °C) δ (ppm):. 150.66, 128.21, 113.90, 55.70, 29.51. MS (ESI): m/z 750,6 [M], 773.5 [M+Na⁺], 789.5 [M+K⁺], 824.6 [M+(CH₃)₄N⁺].

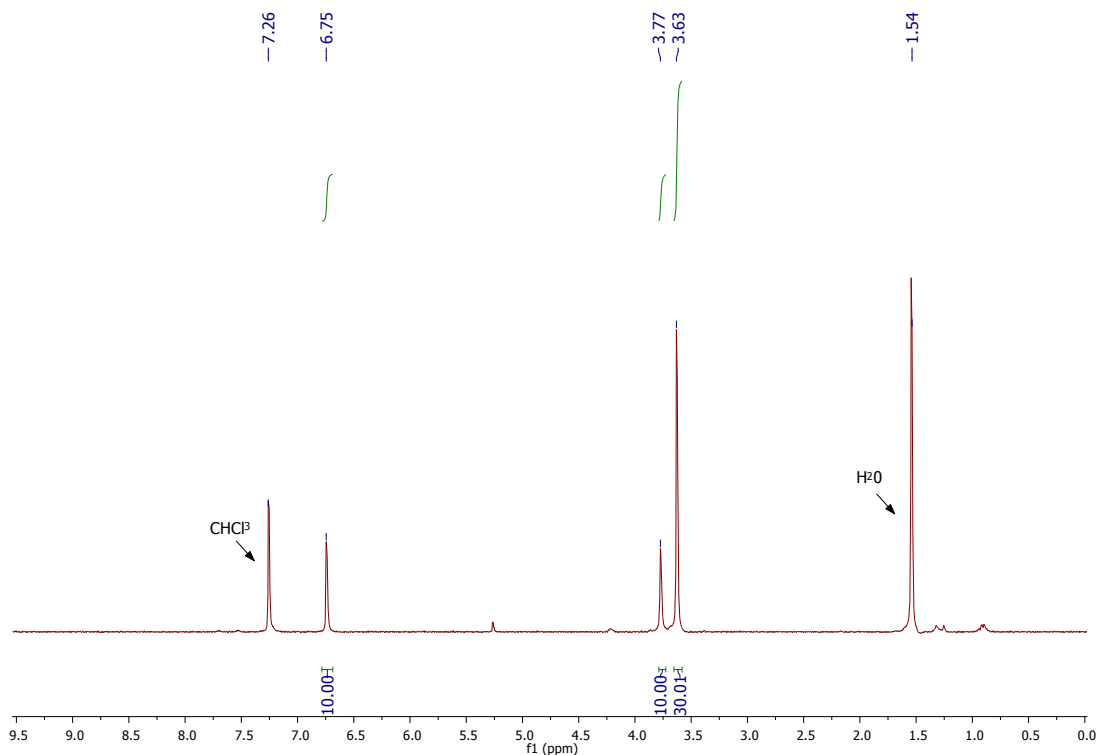


Figure S2. ¹H NMR spectrum of P₁[5]

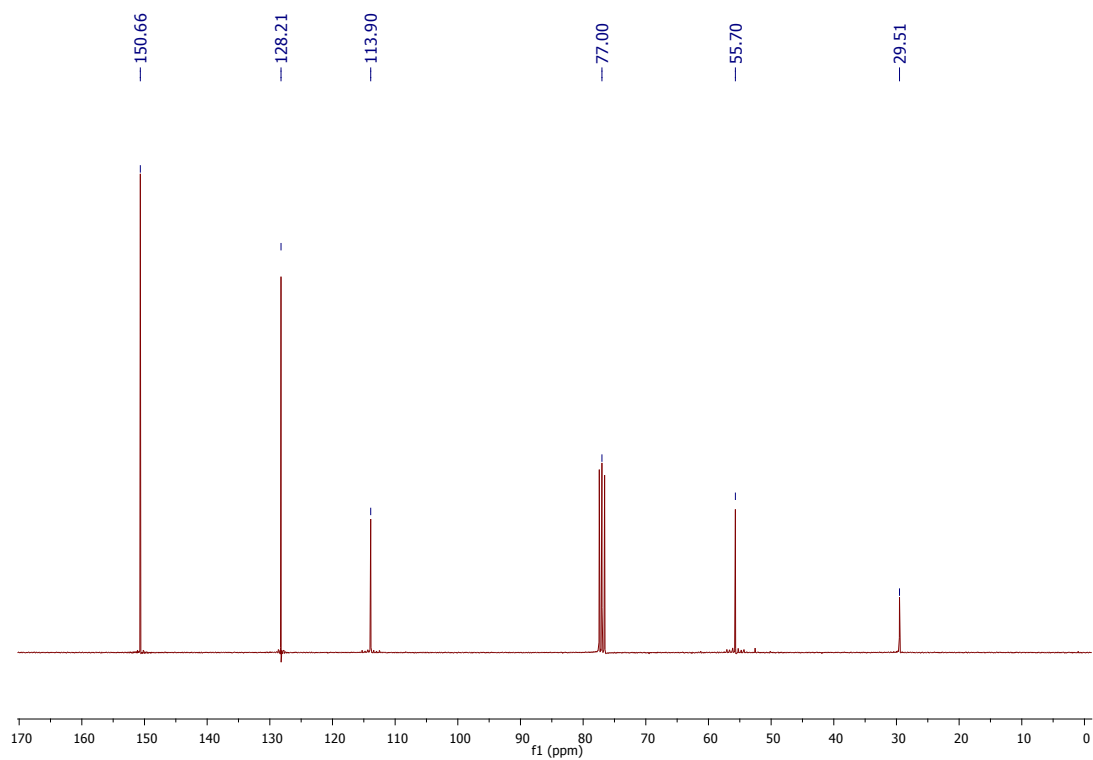


Figure S3. ^{13}C NMR spectrum of $\text{P}_1[5]$

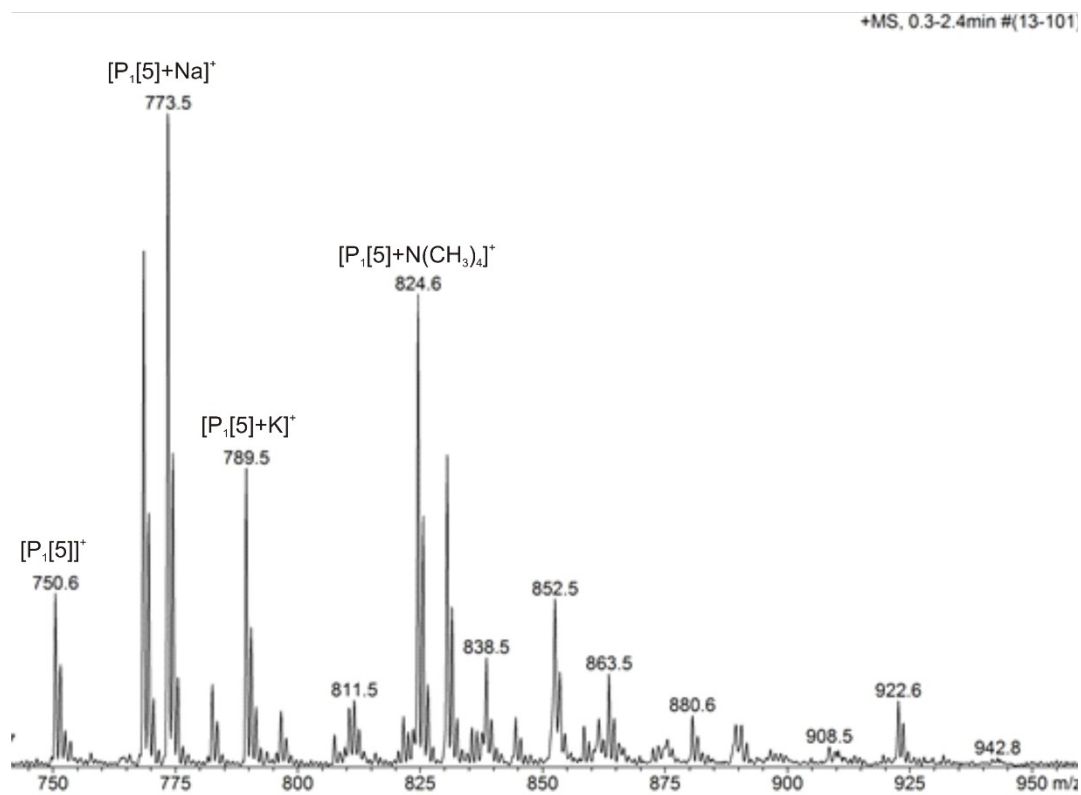
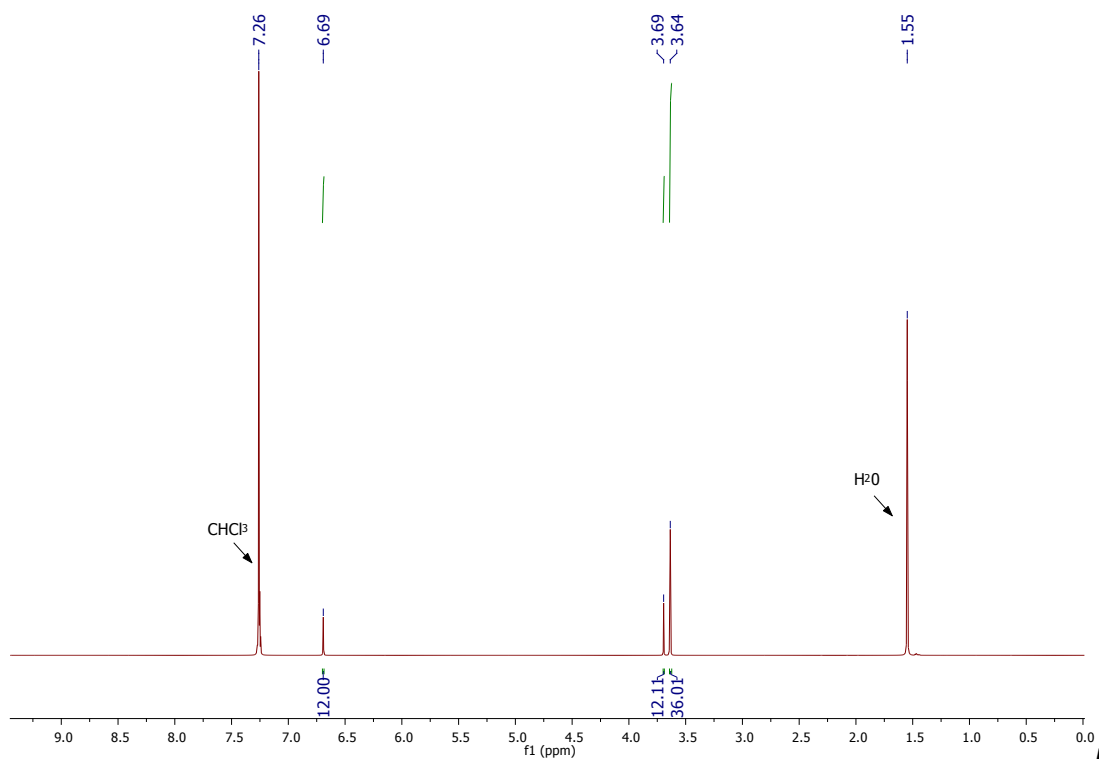


Figure S4. MS (ESI) spectrum of $\text{P}_1[5]$

2.3.2 P₁[6]

¹H NMR (300 MHz, CDCl₃, 25 °C) δ (ppm): 6.69 (s, 12H), 3.69 (s, 12H), 3.64 (s, 36H). ¹³C NMR (300 MHz, CDCl₃, 25 °C) δ (ppm): 151.40, 127.43, 113.59, 56.09, 29.67. MS (ESI): m/z 901,6 [M+H⁺], 918.1 [M+NH₄⁺].



Fig

re S5. ¹H NMR spectrum of P₁[6]

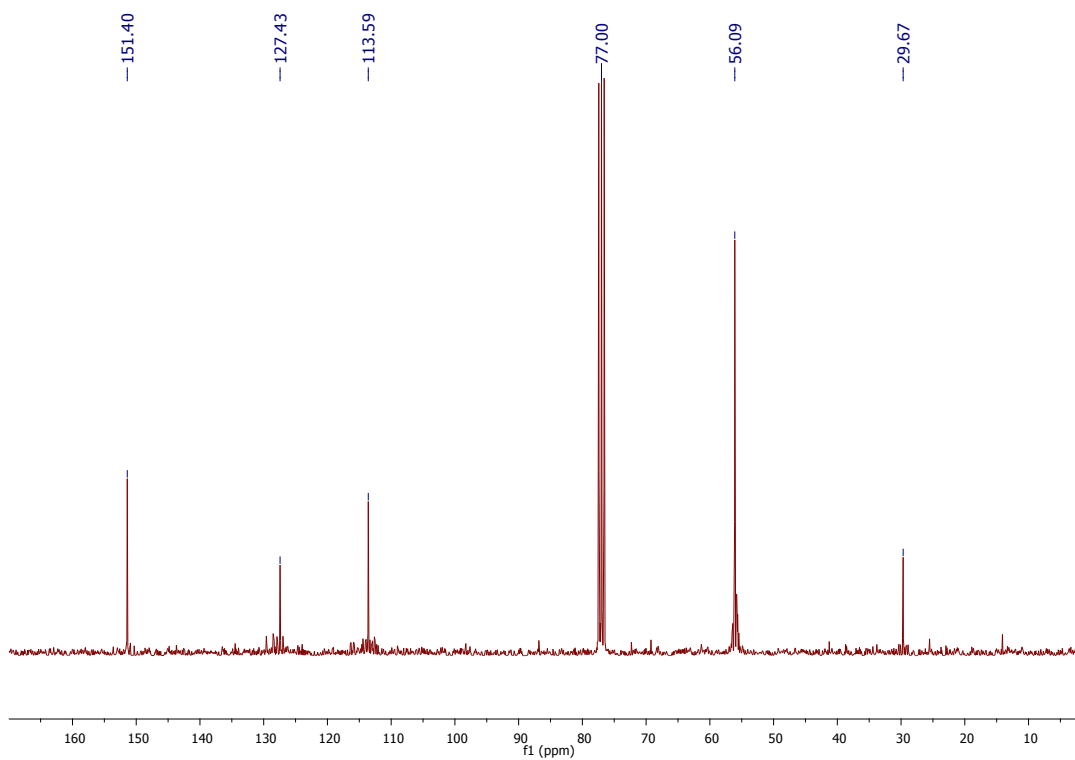


Figure S6. ^{13}C NMR spectrum of $\text{P}_1[6]$

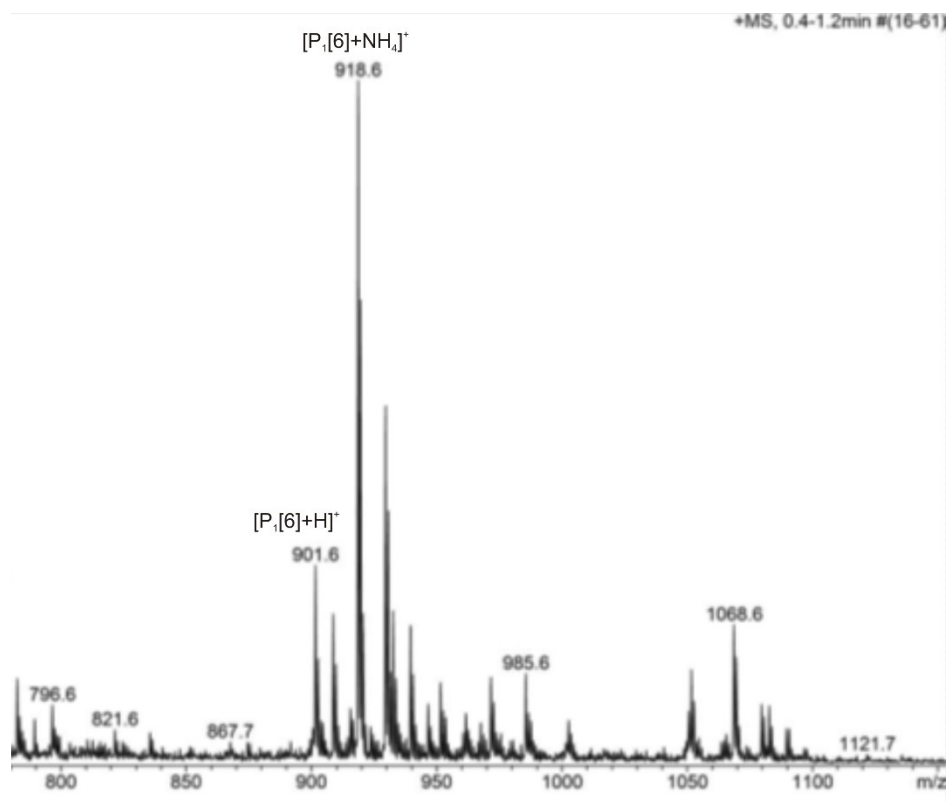


Figure S7. MS (ESI) spectrum of $\text{P}_1[6]$

2.3.3 P₂[5].

¹H NMR (300 MHz, CDCl₃, 25 °C) δ (ppm): 6.72 (s, 10H), 3.81 (q, J = 6Hz, 10H), 3.77 (s, 10), 1.25 (t, J = 6 Hz, 30H). ¹³C NMR (300 MHz, CDCl₃, 25 °C) δ (ppm): 149.81, 128.48, 115.07, 63.74, 29.83, 15.03. MS (ESI): m/z 891.7 [M+H⁺], 908.6 [M⁺+ NH₄⁺], 929.7.6 [M⁺+ K⁺], 964.7 [M⁺+ N(CH₃)₄⁺]

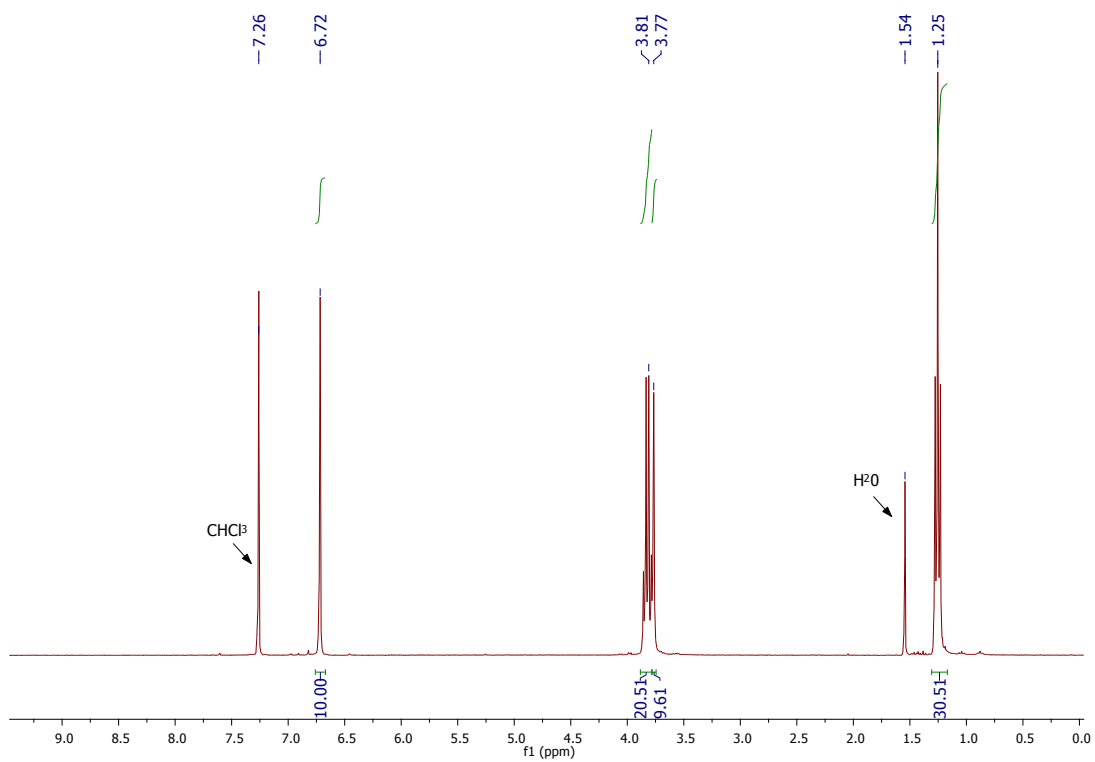


Figure S8. ¹H NMR spectrum of P₂[5]

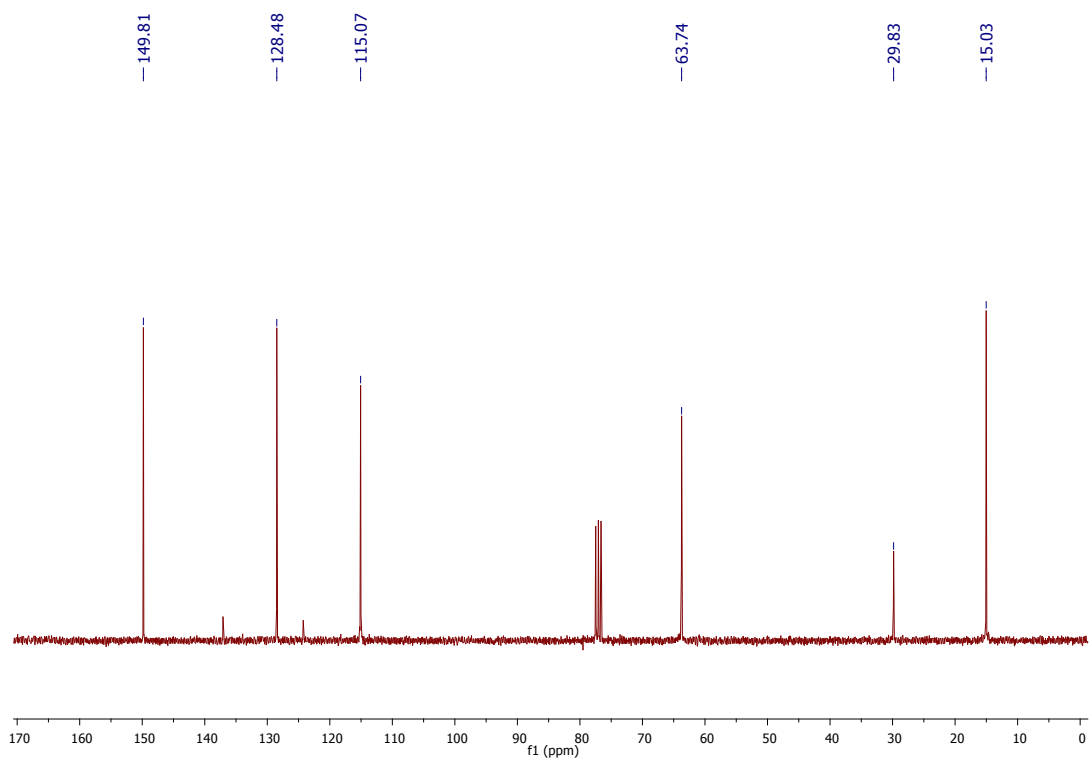


Figure S9. ^{13}C NMR spectrum of $\text{P}_2[5]$

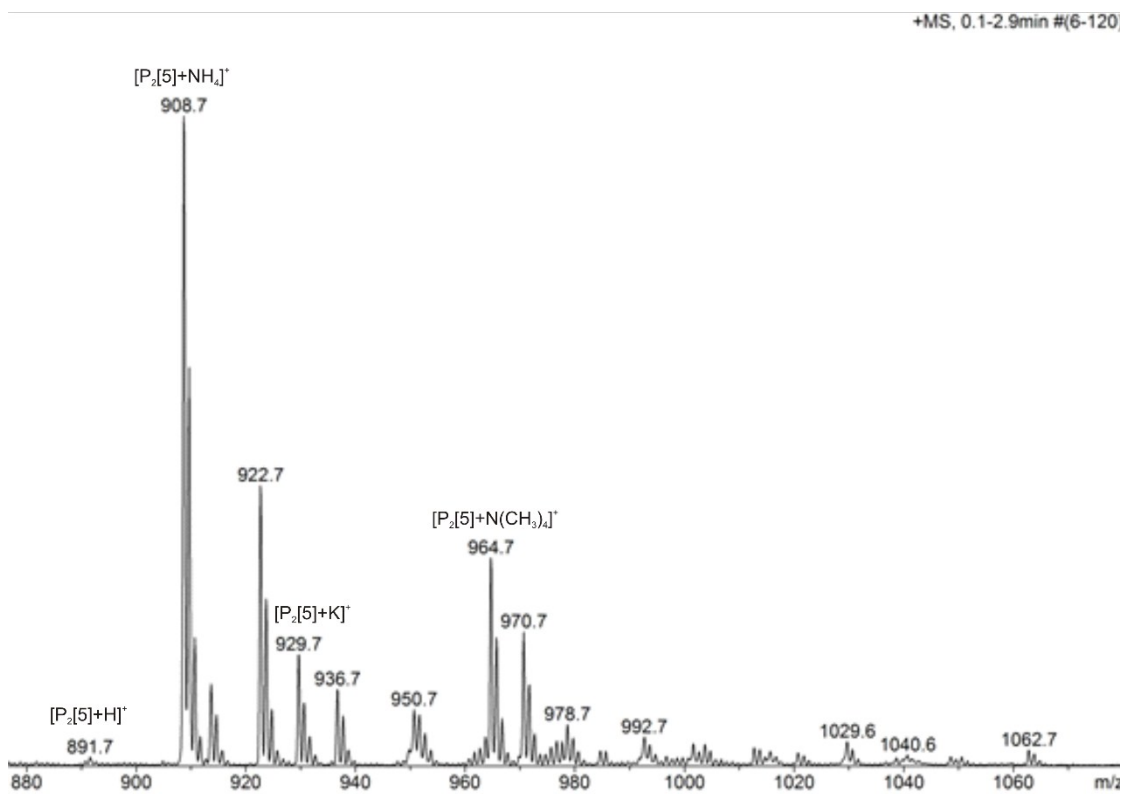


Figure S10. MS (ESI) spectrum of $\text{P}_2[5]$

2.3.4 P₂[6]

¹H NMR (300 MHz, CDCl₃, 25 °C) δ (ppm): 6.69 (s, 12H), 3.80 (q, J = 6Hz, 12H), 3.79 (s, 12H), 1.28 (t, J = 6 Hz, 36H). ¹³C NMR (300 MHz, CDCl₃, 25 °C) δ (ppm): 150.35, 127.78, 115.16, 63.93, 30.86, 15.11. MS (ESI): m/z 1068.9 [M+], 1091.9 [M+Na⁺], 1107.9 [M+K⁺], 1170.9 [M+T₁].

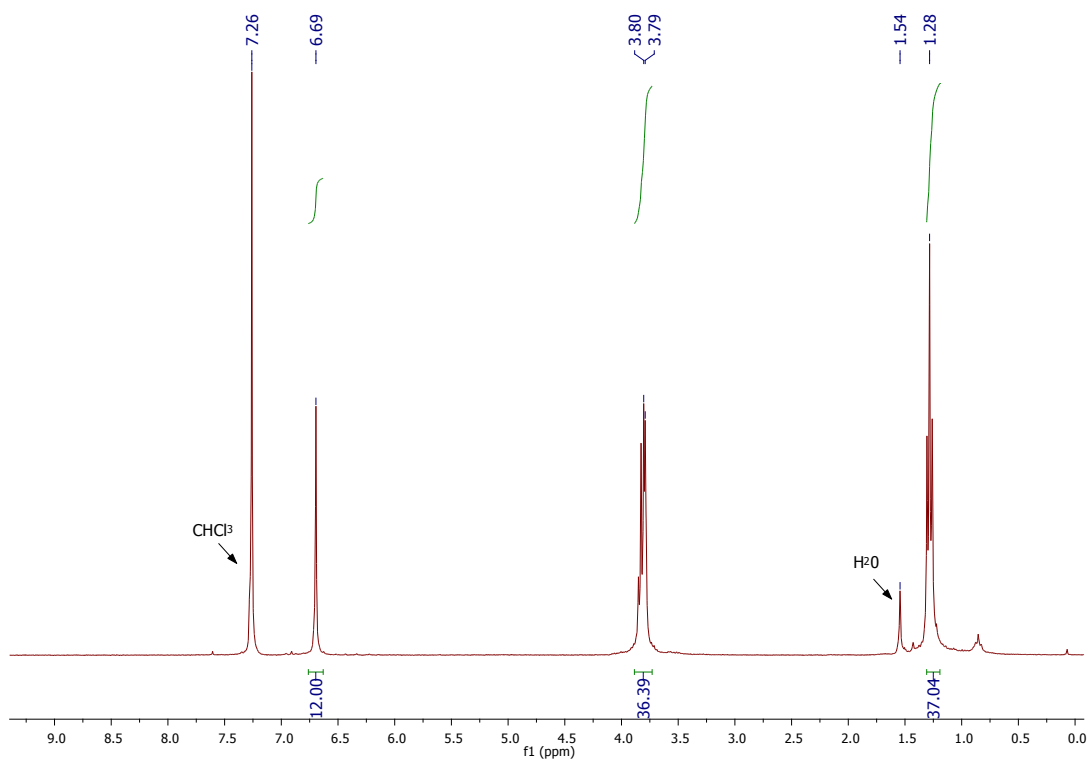


Figure S11. ¹H NMR spectrum of P₂[6]

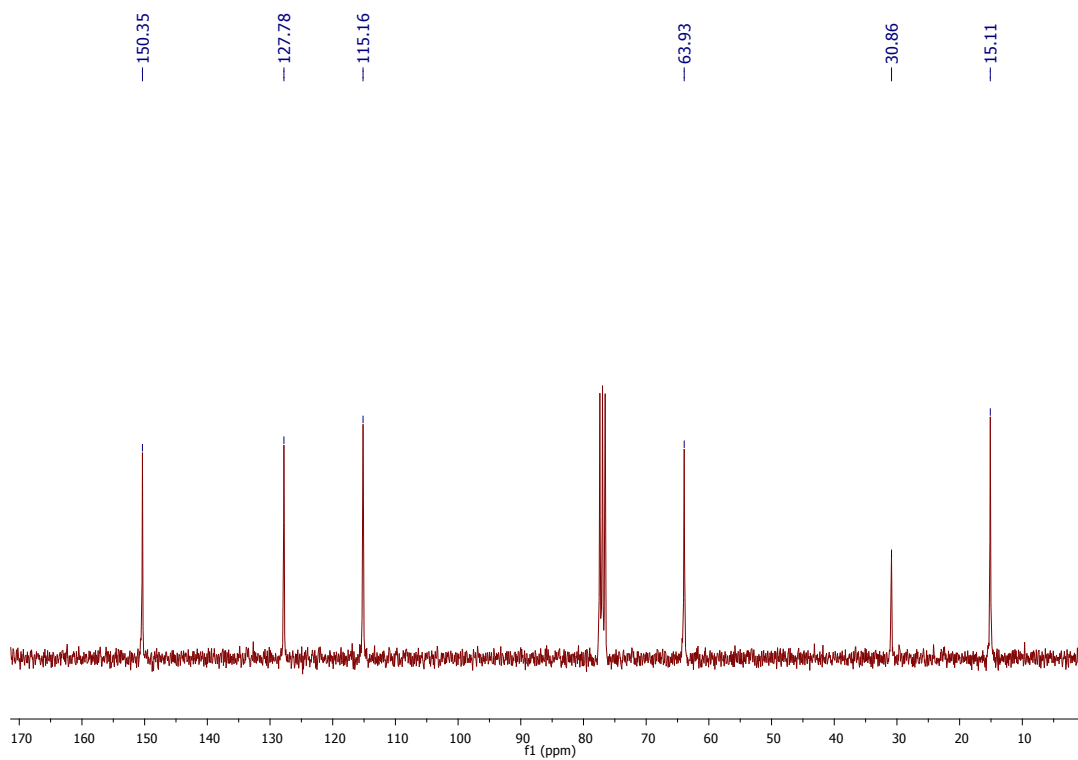


Figure S12. ^{13}C NMR spectrum of $\text{P}_2[6]$

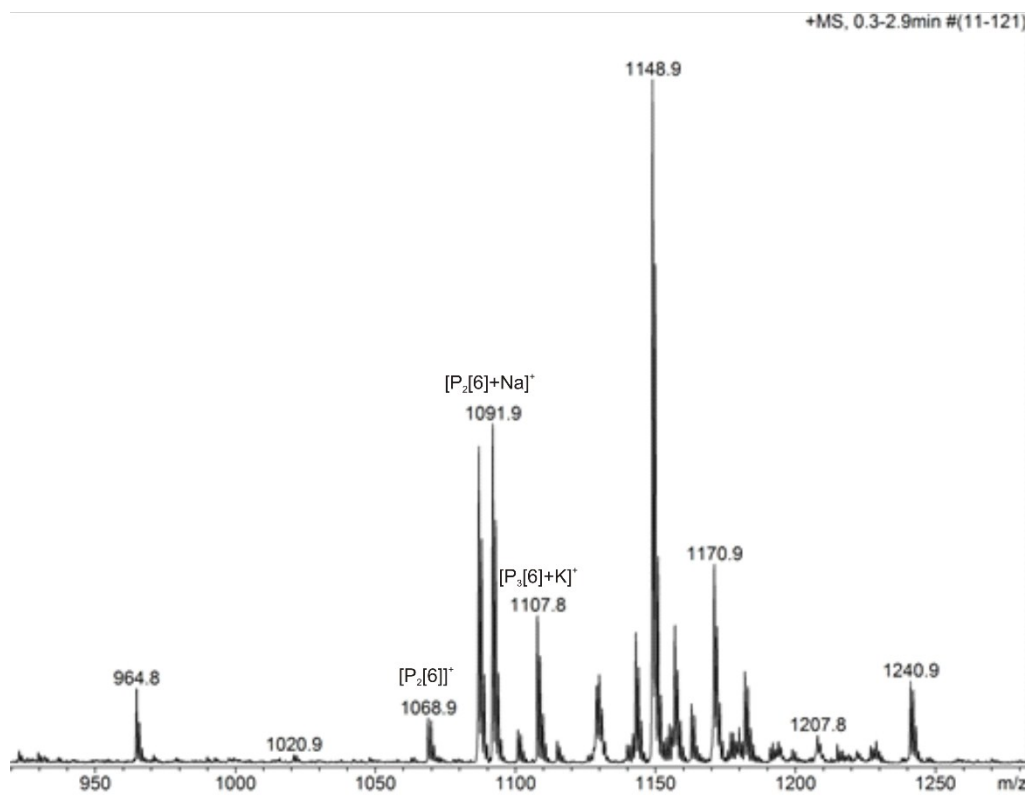


Figure S13. MS (ESI) spectrum of $\text{P}_2[6]$

2.3.5 P₃[5].

¹H NMR (300 MHz, CDCl₃, 25 °C) δ (ppm): 6.92 (s, 10H), 3.93 (t, J = 6Hz, 20H), 3.82 (s, 10H), 1.86 (q, J = 6Hz, 20H), 1.59 (s, J = 6Hz, 20H), 1.05 (t, 30H). ¹³C NMR (300 MHz, CDCl₃, 25 °C) δ (ppm): 149.74, 128.15, 114.64, 67.90, 32.03, 29.33, 19.51, 14.02. MS (ESI): m/z 1171.1[M+H⁺], 1189.2 [M+NH₄⁺], 1210.1 [M+K⁺].

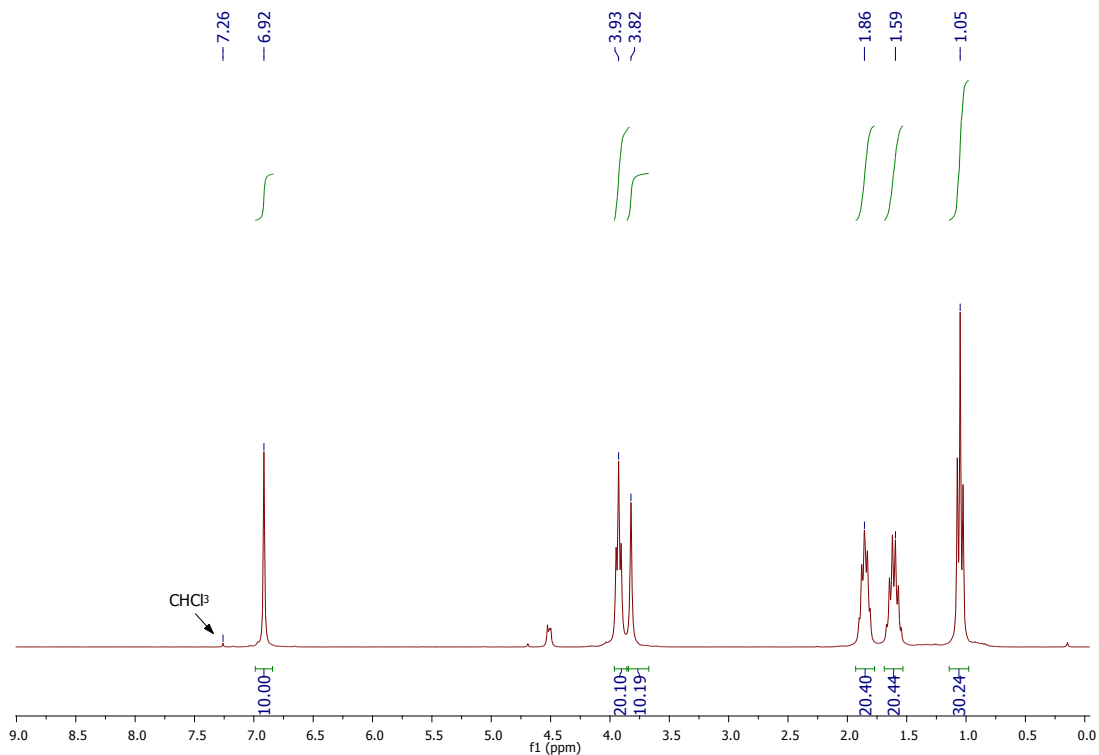


Figure S14. ¹H NMR spectrum of P₃[5]

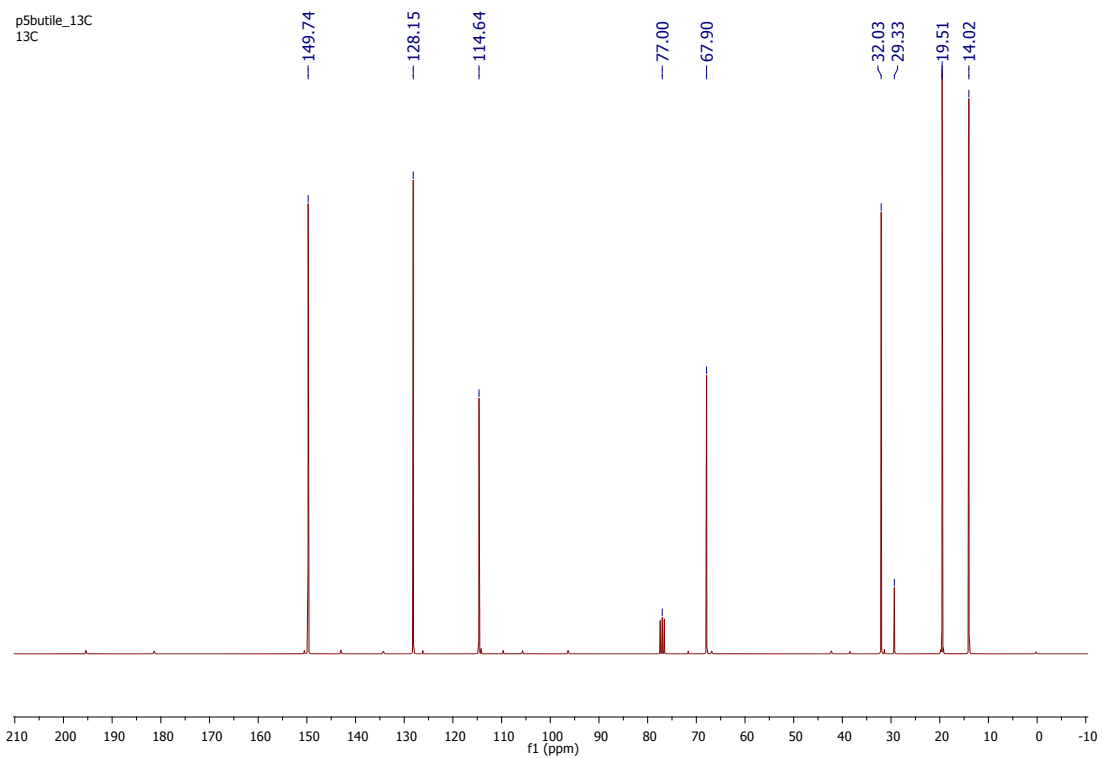


Figure S15. ^{13}C NMR spectrum of $\text{P}_3[5]$

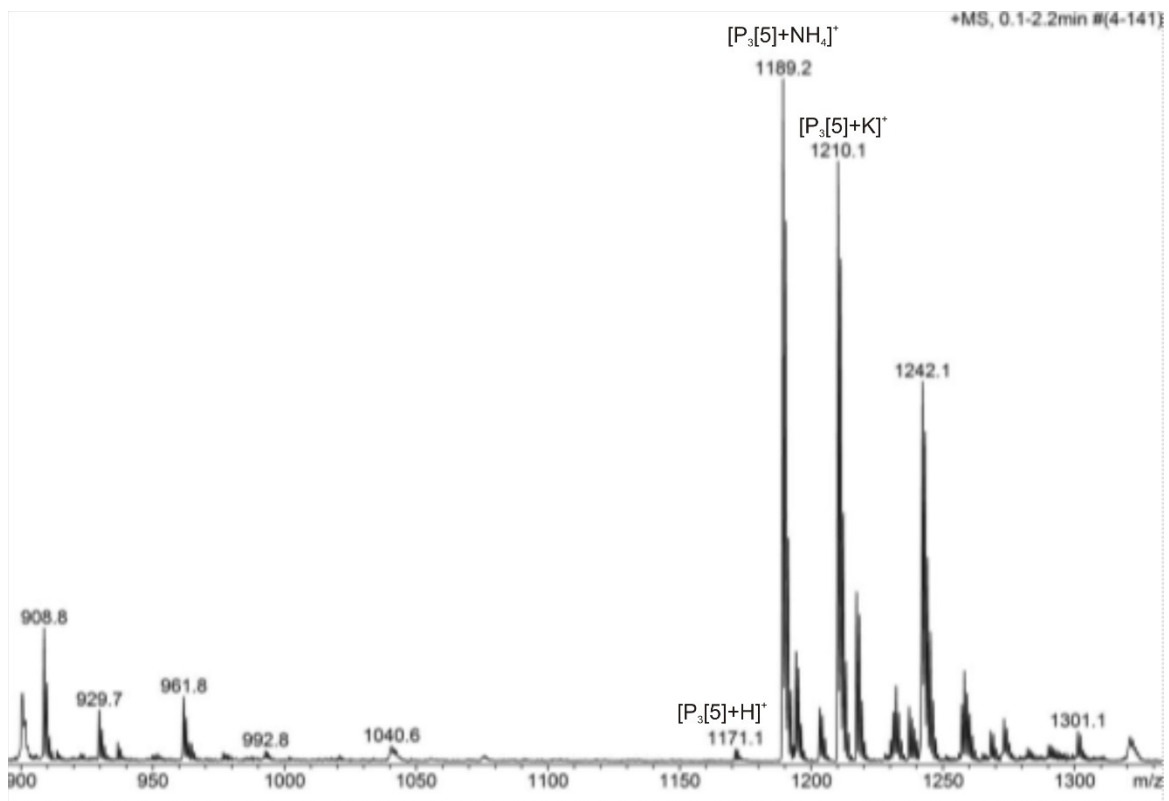


Figure S16. MS (ESI) spectrum of $\text{P}_3[5]$

2.3.6 P₃[6]

¹H NMR (300 MHz, CDCl₃, 25 °C) δ (ppm): 6.69 (s, 12H), 3.76 (t, J = 6Hz, 24H), 3.76 (s, 12H), 1.69 (q, J = 6Hz, 24H), 1.42 (s, J = 6Hz, 24H), 0.91 (t, 36H). ¹³C NMR (300 MHz, CDCl₃, 25 °C) δ (ppm): 150.41, 127.80, 114.93, 68.17, 31.87, 30.70, 19.39, 13.90. MS (ESI): m/z 1423.4[M+NH₄⁺], 1477.3 [M+N(CH₃)₄⁺].

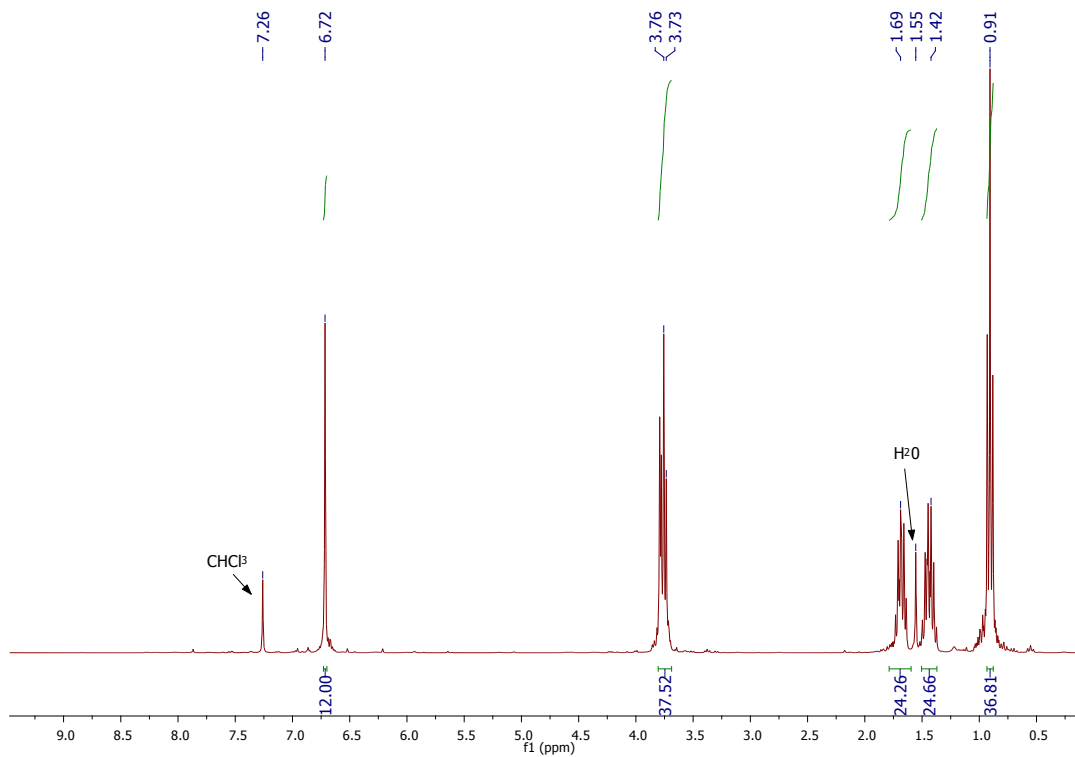


Figure S17. ¹H NMR spectrum of P₃[6]

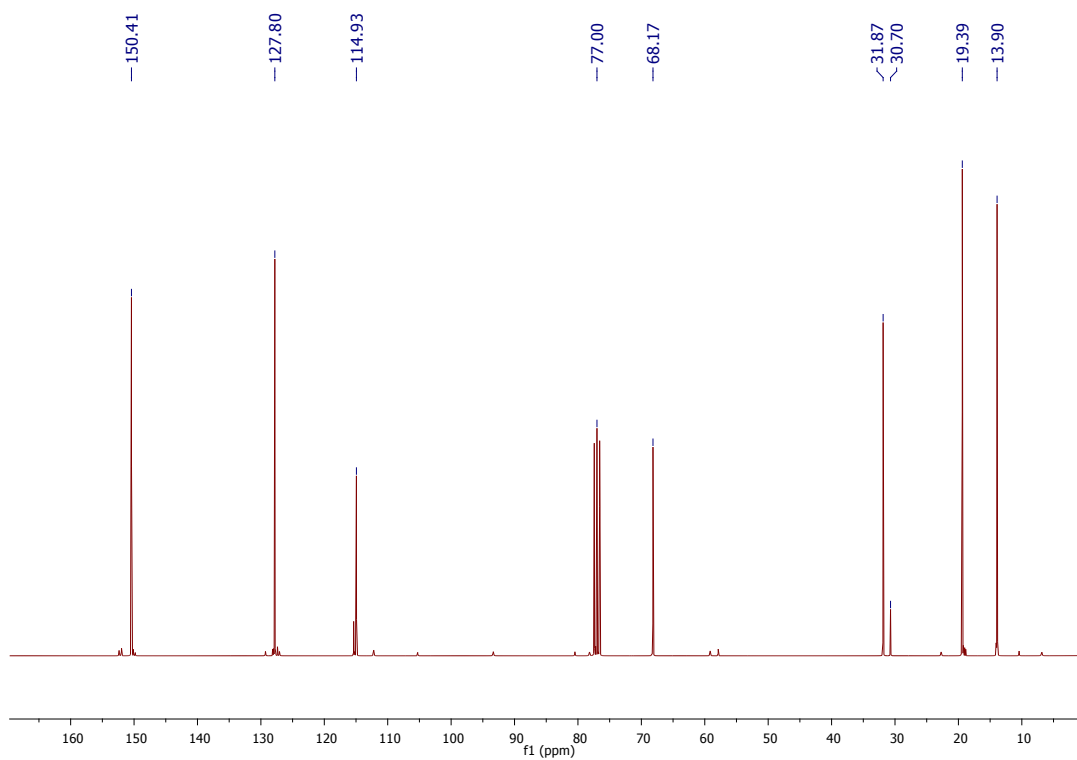


Figure S18. ^{13}C NMR spectrum of $\text{P}_3[6]$

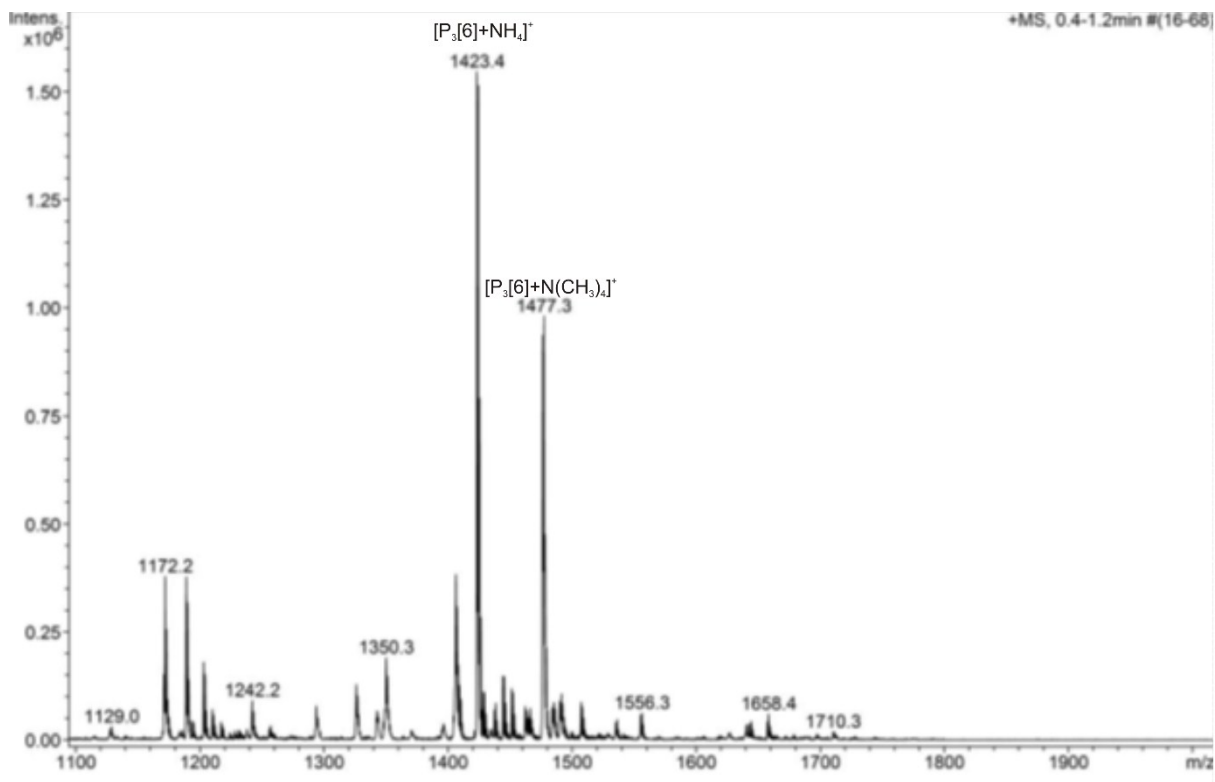


Figure S19. MS (ESI) spectrum of $\text{P}_3[6]$

3. ^1H NMR Spectra of Host-Guest Interaction of $\text{P}_2[5]$ with T_2 , T_3 , T_4

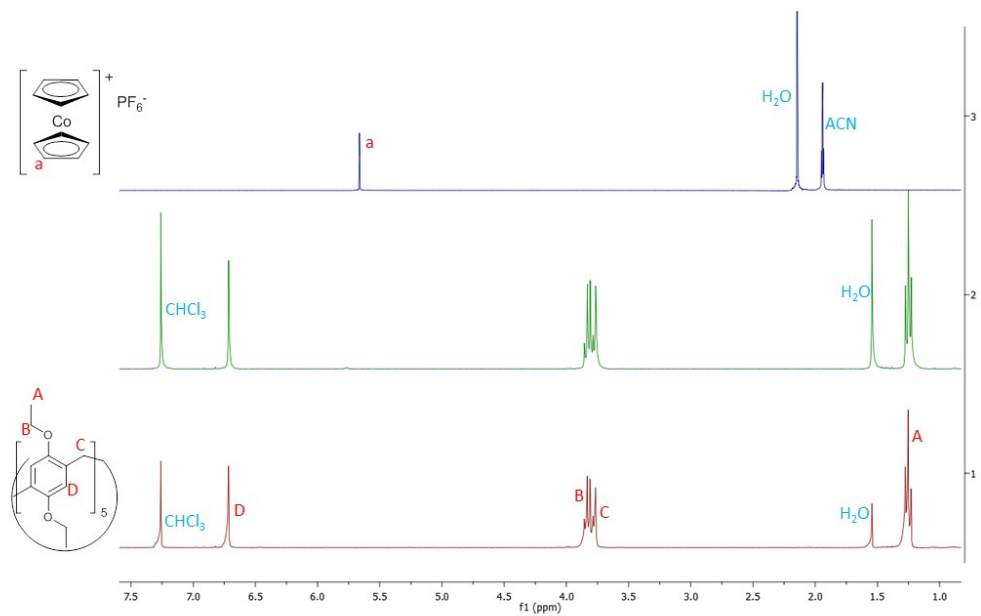


Figure S20. ^1H NMR spectrum of host-guest interaction of $\text{P}_2[5]$ with T_2

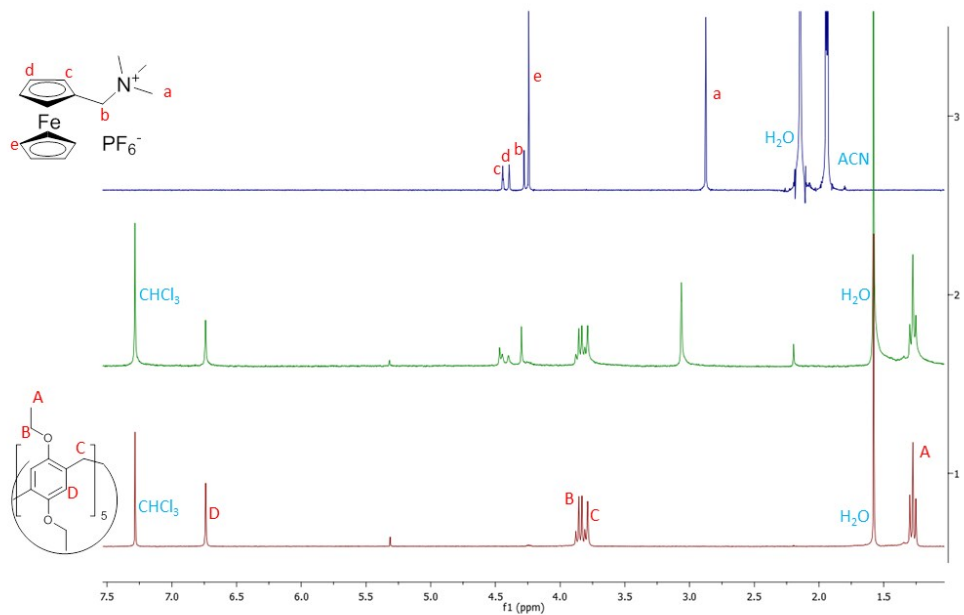


Figure S21. ^1H NMR spectrum of host-guest interaction of $\text{P}_2[5]$ with T_3

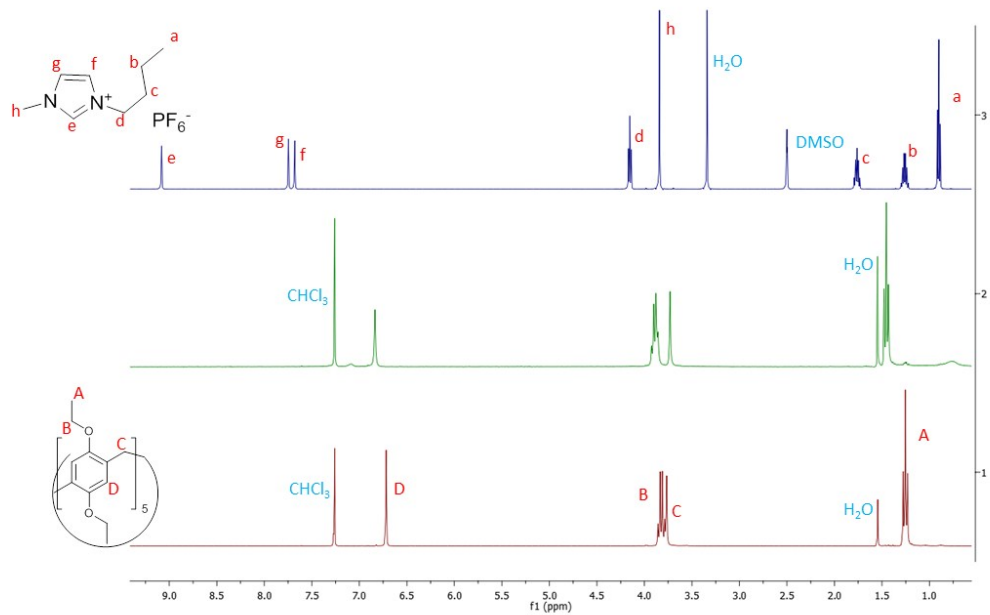


Figure S22. ^1H NMR spectrum of host-guest interaction of $\text{P}_2[5]$ with T_4

4. ^1H NMR Spectra of Host-Guest Interaction of $\text{P}_2[6]$ with T_2 , T_3 , T_4

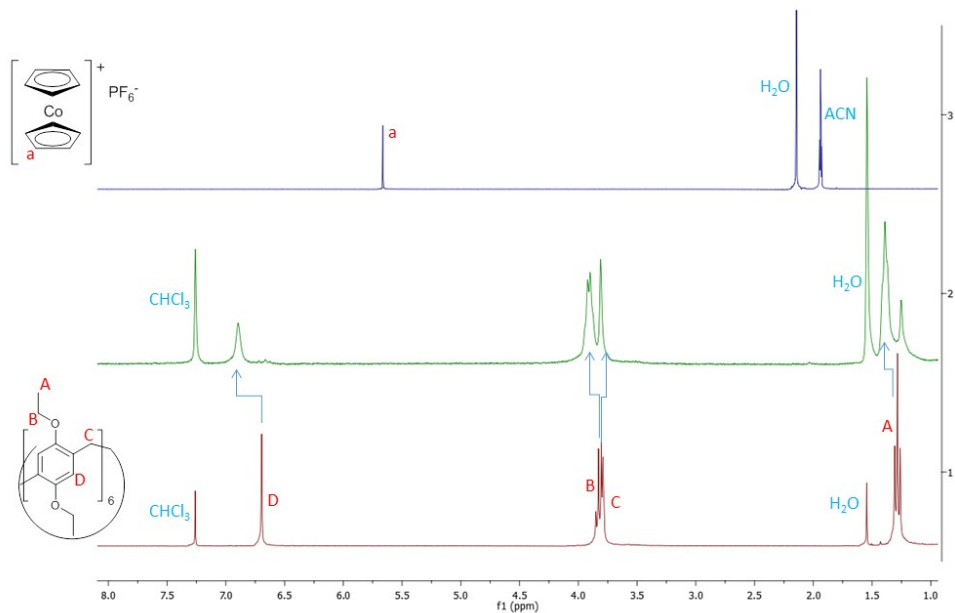


Figure S23. ^1H NMR spectrum of host-guest interaction of $\text{P}_2[6]$ with T_2

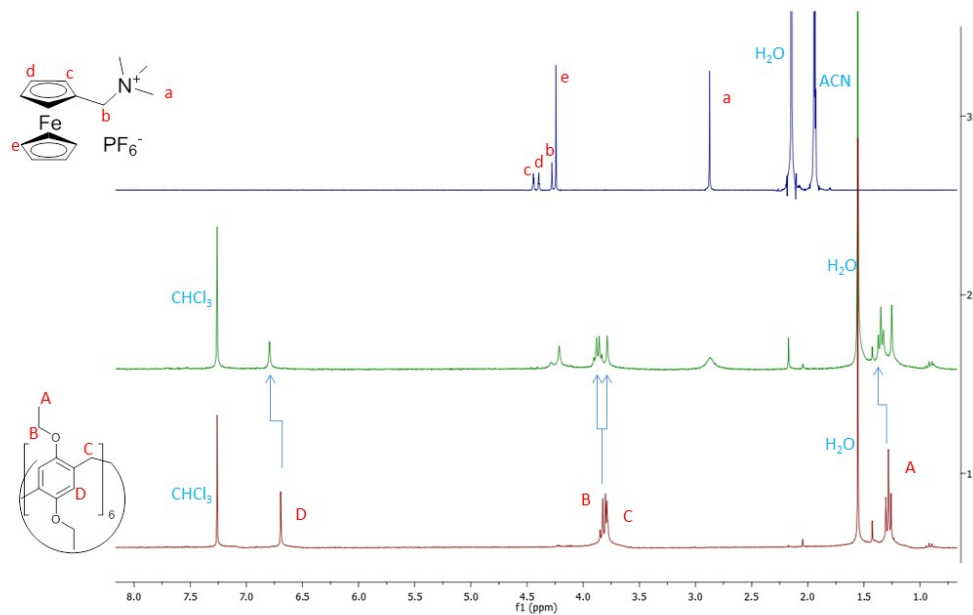


Figure S24. ^1H NMR spectrum of host-guest interaction of $\text{P}_2[6]$ with T_3

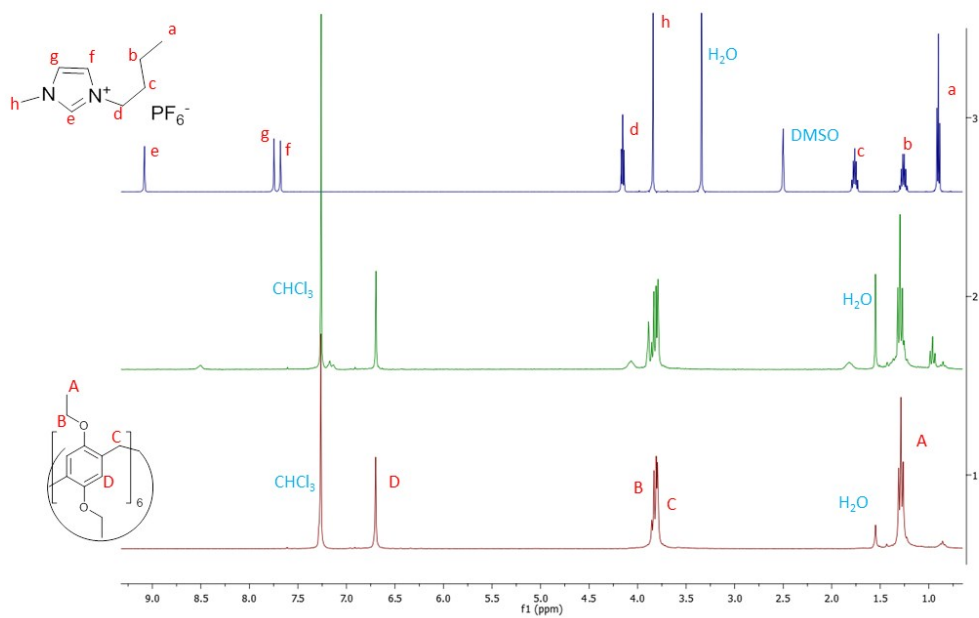


Figure S25. ^1H NMR spectrum of host-guest interaction of $\text{P}_2[6]$ with T_4

5. ESI-MS Spectra of Host-Guest complex of P₂[5] with T₄

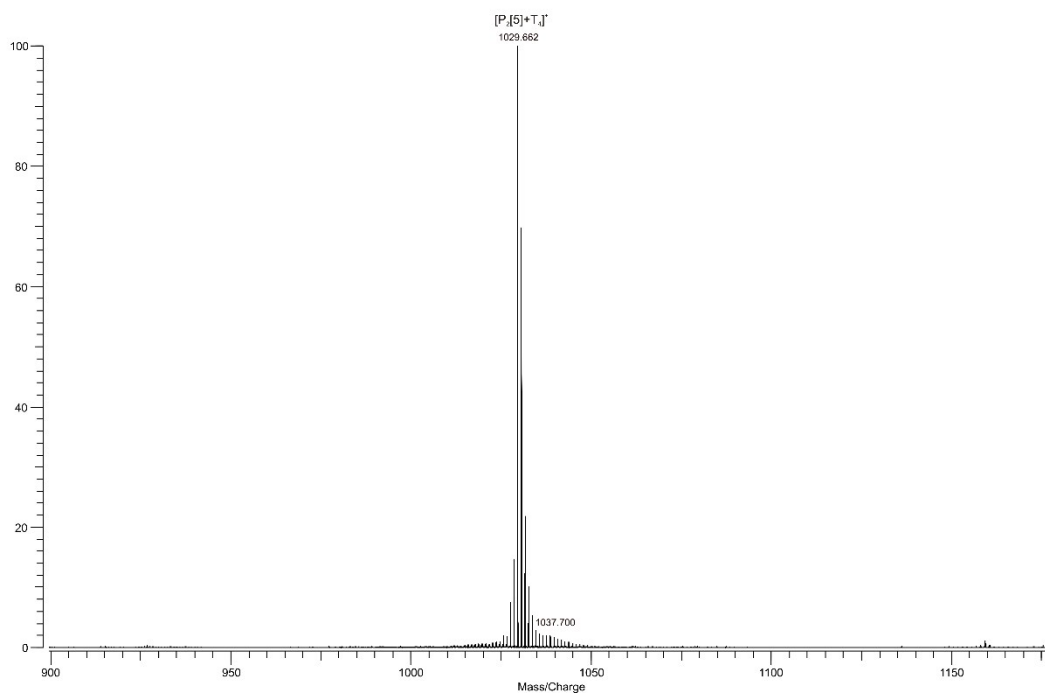


Figure S26. MS (ESI) spectrum of P₂[5] + T₄, m/z 1029.7.

6. ESI-MS Spectra of Host-Guest complex of P₂[6] with T₂, T₃.

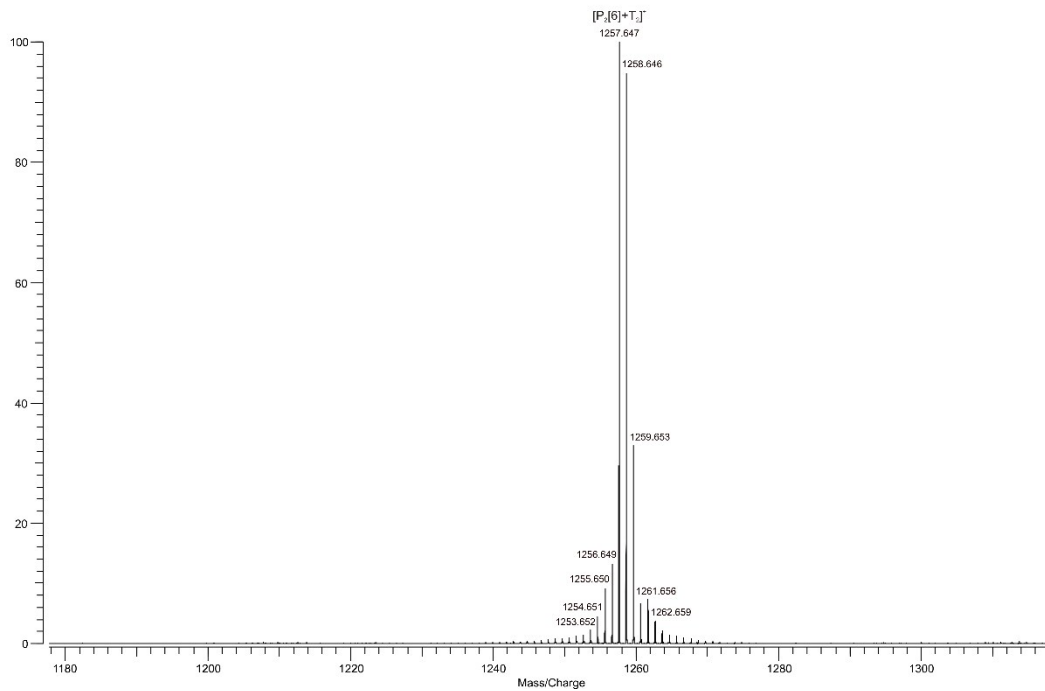


Figure S27. MS (ESI) spectrum of P₂[6] + T₂, m/z 1257.6.

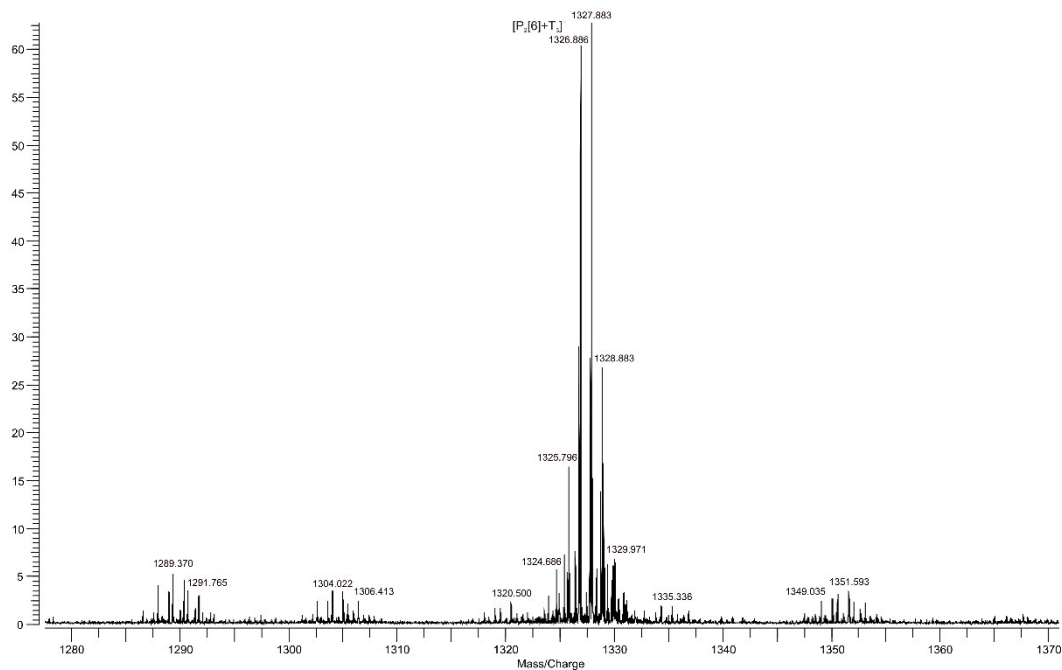


Figure S28. MS (ESI) spectrum of $P_2[6] + T_3$, m/z 1326.9.

7. Determination of the Kass between $P_2[6]$ and T_2

$P_2[6]$ was dissolved in $CDCl_3 : ACN-d_3$ 1:1 to obtain a 2 mM solution. T_2 was dissolved in $CDCl_3 : ACN-d_3$ 1:1 to obtain a 40 mM solution. 1 mL of $P_2[6]$ solution was poured into the NMR tube and the first spectrum recorded. T_2 solution was added in amounts from 5 μ L to 50 μ L each time, recording spectra after each addition, until the amount of guest present in solution was 5 times more than the host one.

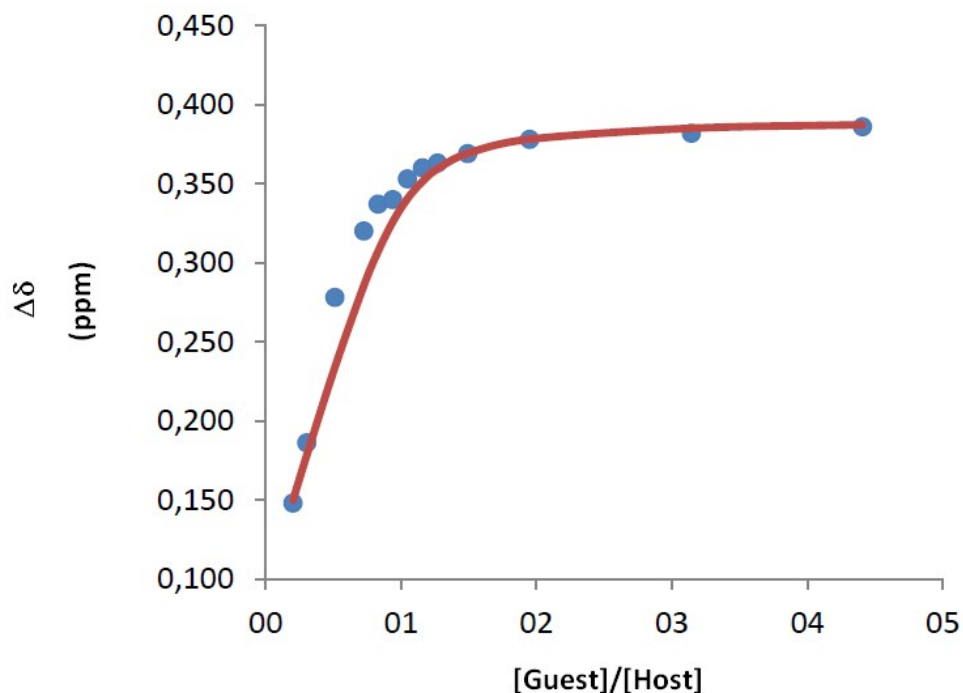


Figure S29. Plot for the titration of $P_2[6]$ with T_2 and fitting of the data for the calculation of the K_{ass} ($1.2 \cdot 10^4 M^{-1}$).

8. Semiempirical PM3 model calculations on $T_2@P_2[5]$ and $P_2@P_2[6]$

Molecular modelling (semi-empirical PM3 calculations) of $T_2@P_2[5]$ and $T_2@P_2[6]$ shows that can explain what observed experimentally. Indeed, the templating molecule T_2 barely fits in the cavity of $P_2[5]$, and the analysis of the model displays that bumps (close inter-atomic contacts between atoms that are within 70% of the sum of the covalent radii) can only avoided by forcing cobaltocenium into a nearly eclipsed conformation, enhancing the overall energy of the structure itself. On the contrary, the larger cavity of $P_2[6]$ allows the more favoured staggered conformation of T_2 , without contacts with the inner walls of the cavity.

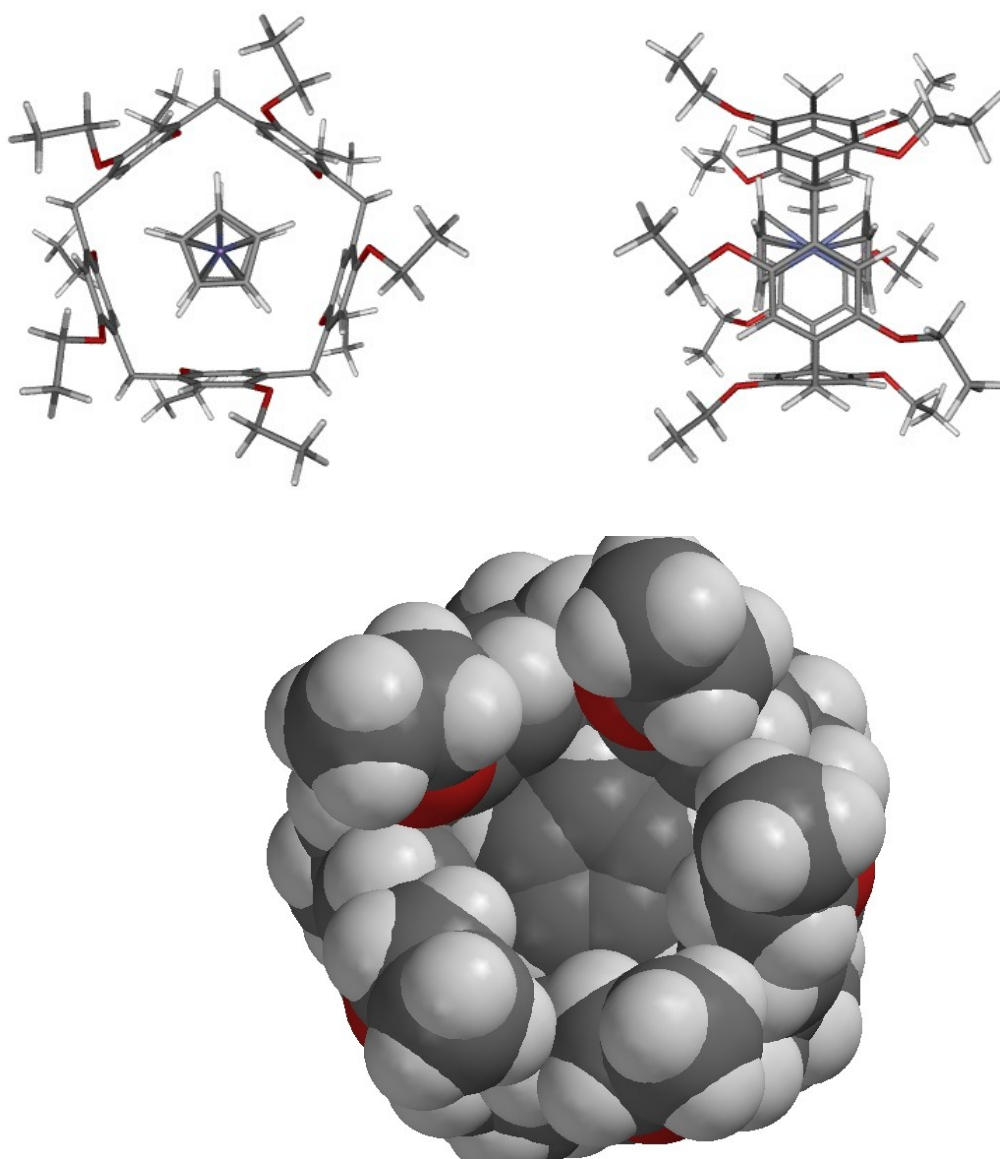


Figure S30. Minimized (semiempirical PM3) structure of **T2@P₂[5]** on top (left: front view; right: lateral view) and space filling structures bottom (front view).

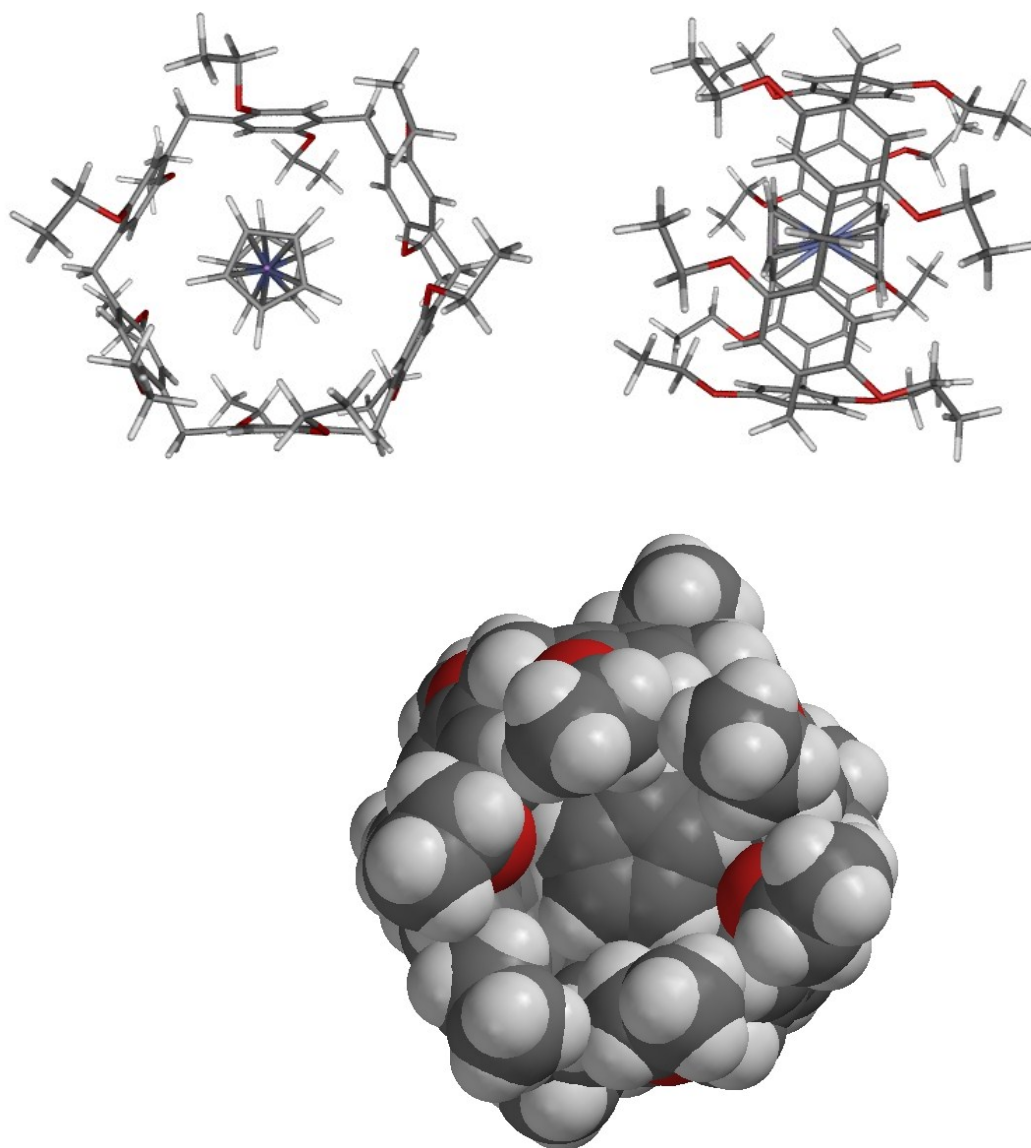


Figure S31. Minimized (semiempirical PM3) structure of **T2@P₂[6]** on top (left: front view; right: lateral view) and space filling structures bottom (front view).

A plot of the calculated energies (semi-empirical PM3) of **P₂[5]** and **P₂[6]** with cobalt atom of **T2** "frozen" at increasing distance from the centre of cavities is reported.

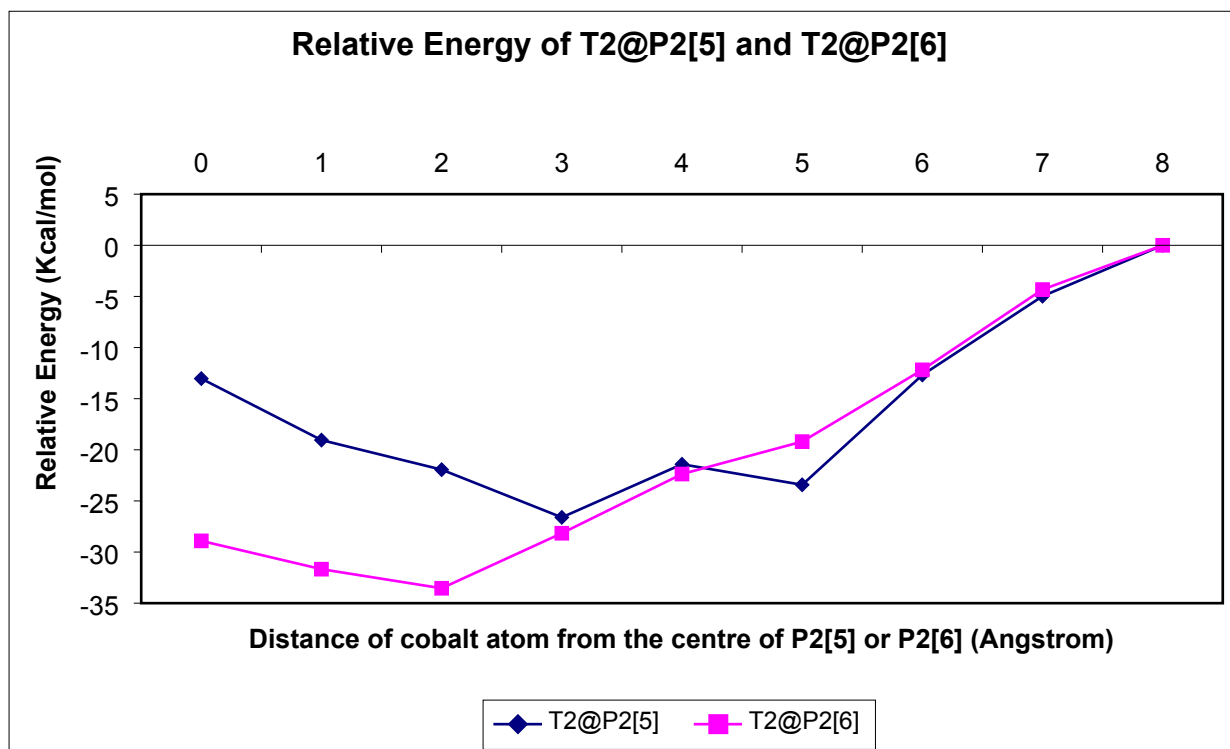


Figure S32. Plot of the relative energy for the **T2@host** systems as function of the distance between the centers of mass of the host and the guest **T2**.

The plot displays in both cases a gain of energy when the host enters both cavities (the energy level 0 was arbitrary set at 8 Å for both structures), and the **T2@P₂[6]** inclusion process results more exothermic.

References

- S1. J.K. Lindsay, C.R. Hauser, *J. Org. Chem.*, 1957, **22**, 355.
- S2. R.A.W. Johnston, M.E. Rose, *Tetrahedron* 1979, **35**, 2169.